INTERNATIONAL JOURNAL OF ROBUST AND NONLINEAR CONTROL
Int. J. Robust Nonlinear Control 2009; **19**:92–116
Published online 22 July 2008 in Wiley InterScience (www.interscience.wiley.com). DOI: 10.1002/rnc.1340

Linear parameter varying control of wind turbines covering both partial load and full load conditions

Kasper Zinck Østergaard[1,*,†], Jakob Stoustrup[2] and Per Brath[1]

[1]*Turbine Control and Operation R&D, Vestas Wind Systems A/S, Alsvej 21, 8900 Randers, Denmark*
[2]*Automation and Control, Department of Electronic Systems, Aalborg University, Fredrik Bajers Vej 7C, 9220 Aalborg Ø, Denmark*

SUMMARY

This paper considers the design of linear parameter varying (LPV) controllers for wind turbines in order to obtain a multivariable control law that covers the entire nominal operating trajectory.

The paper first presents a controller structure for selecting a proper operating trajectory as a function of estimated wind speed. The dynamic control law is based on LPV controller synthesis with general parameter dependency by gridding the parameter space.

The controller construction can, for medium- to large-scale systems, be difficult from a numerical point of view, because the involved matrix operations tend to be ill-conditioned. The paper proposes a controller construction algorithm together with various remedies for improving the numerical conditioning the algorithm.

The proposed algorithm is applied to the design of a LPV controller for wind turbines, and a comparison is made with a controller designed using classical techniques to conclude that an improvement in performance is obtained for the entire operating envelope. Copyright © 2008 John Wiley & Sons, Ltd.

Received 1 August 2007; Revised 4 April 2008; Accepted 7 April 2008

KEY WORDS: linear parameter varying control; control of wind turbines; gain scheduling; numerical conditioning

1. INTRODUCTION

In the wind energy industry, there has been a large focus on increasing the capacity of wind turbines in order to reduce the installation costs when compared with the power production during the lifetime of the wind turbine. This has resulted in a rapid growth in rotor size and electrical power production, and in the period from 1980 to 2003 the largest wind turbine size has grown from approximately 50 to 5000 kW, which is more than a 20% increase per year for more than 20 years [1].

*Correspondence to: Kasper Zinck Østergaard, Turbine Control and Operation R&D, Vestas Wind Systems A/S, Alsvej 21, 8900 Randers, Denmark.
†E-mail: kasper@zincke.dk

This dramatic increase in wind turbine size and capacity has made it very challenging to design wind turbines, because many of the structural and electrical components are not scalable, i.e. the costs introduced by scaling the components grow at a higher rate than the benefits from increased production. For the structural components, this means that the components must be made lighter without compromising their durability, e.g. by improving the performance of active control.

Previous investigations such as [2–6] have shown that linear, time-invariant methods provide good closed-loop results when observing local behaviour. A natural choice for controller design covering the entire operating envelope is therefore to design linear controllers along a chosen operating trajectory and then to interconnect them in an appropriate way in order to get a control formulation for the entire operating region. This approach is denoted as gain scheduling and in [7–9] this is done by interpolating the outputs of a set of local controllers (either by linear interpolation or by switching). Alternatively, parameters of the controller are updated according to a pre-specified function of a measured/estimated variable [10–12].

A systematic way of designing such parameter-dependent controllers is within the framework of linear parameter varying (LPV) systems. Here, the model will be represented by a linear model at all operating conditions and a controller with similar parameter dependency is synthesized to guarantee a certain performance specification for all possible parameter values within a specified set. A major difference to classical gain scheduling is that it is possible to take into account that the scheduling parameters can vary in time. In this paper we will, due to numerical considerations, assume arbitrary fast parameter variations, which is the most restrictive form of LPV control.

In [13–15] the LPV design procedure is applied for the special case of affine parameter dependency. However, affine parameter dependency is a very strict requirement for designing controllers for wind turbines in the entire operating region. Mainly because the performance criteria are very different in partial load when compared with full load control, but also because it is rather crude to approximate the nonlinear aerodynamics by a first-order function over the entire operating region. In [13, 14] this is handled by designing different LPV controllers for the below- and above-rated wind speeds and then switching between them.

The gain-scheduled design methods in the literature consider one controller for partial load and another controller for full load operation (except for [15] in which a simplistic parameter dependency is assumed). This means that a method for bumpless transfer between two very different controllers needs to be implemented to make the control law work in practice. In this paper we consider an alternative approach in which a gain-scheduled controller is designed for both partial load and full load operations for a 3 MW wind turbine with a rotor diameter of 90 m.

As performance criteria, the design will focus on tracking a generator speed reference together with minimization of fatigue damage in vital components, e.g. drive train and tower. Control effort is also taken into account to avoid the pitch system to wear out and the power fluctuations to be too high. In order to handle the very different performance criteria for low wind speeds and high wind speeds, it has been decided to use a grid-based method as in [16], because it makes it possible to use a general form of parameter dependency. The controller construction is very sensitive to numerical issues and a number of remedies are presented for conditioning the construction procedure. To reduce numerical complexity, it has been decided to focus only on arbitrary fast parameter variations throughout the paper.

The paper is structured as follows. In Section 2 we discuss the closed-loop objectives that will be considered in the design process and in Section 3 the considered wind turbine model is presented. A controller structure is given in Section 4 for tracking the desired target trajectory. This section is followed by a presentation of the performance channel for the LPV design in Section 5. Then in

DOI: 10.1002/rnc

Section 6 the LPV controller design method is presented and a discussion of numerical remedies for controller construction is made in Section 7. In Section 8 closed-loop simulation results are presented and conclusions are given in Section 9.

2. CONTROL OBJECTIVES

The main objective for wind turbine controllers is to maximize the trade-off between the annual energy production and the construction and maintenance costs of the wind turbine. This has resulted in two operational modes for pitch-regulated variable-speed wind turbines: partial load and full load operations.

Partial load operation is the mode in which there is not enough kinetic energy in the wind to achieve nominal electrical power production. In this mode the primary objective is to control the pitch and rotor speed to achieve the maximum aerodynamic efficiency of the wind turbine.

Full load operation is the mode in which the kinetic energy in the wind field has exceeded the nominal electrical power production and conversion losses. In this mode the generator speed should be kept close to the nominal speed and the pitch angle should be controlled to achieve nominal electrical power production. Further, it is important to reduce the fluctuations on the power, known as flicker.

In both operating regions, it is important to minimize the fatigue loads in critical structural components, and in this paper the following three components will be considered: drive train, tower in the fore–aft direction, and pitch system.

In addition, it is crucial that the generator speed does not exceed the maximum generator speed in order not to overheat the electrical components. When combining these conditions, the steady-state trajectory of the wind turbine can be described by a function of wind speed, which is illustrated in Figure 1. The requirements regarding optimization of power production and deviations from nominal generator speed then amount to tracking the steady-state trajectory in Figure 1 as closely as possible.

The other performance criteria can be seen as detuning of the tracking controller to limit structural oscillations and high amounts of control effort. For the pitch activity, it is well known that during high wind speeds a high amount of activity is required to track the target trajectory and minimize tower loads. During low wind speeds, the pitch angle should be kept close to the value yielding maximum aerodynamic performance. This means that there needs to be a high emphasis on the wear in the pitch system during low wind speeds, whereas higher variations can be tolerated during high wind speeds.

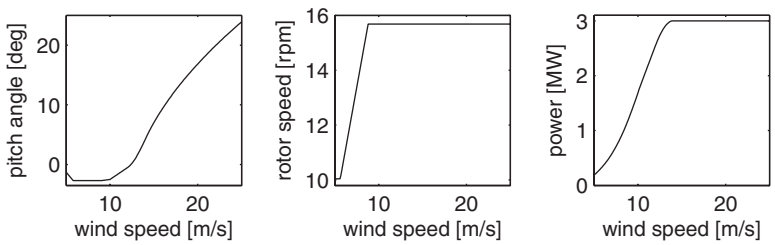

Figure 1. Illustration of operating region for wind turbine.

DOI: 10.1002/rnc

As discussed above, the requirements are different for low wind speeds and high wind speeds. This is not only in terms of use of the control signals, but also for fatigue loads and tracking performance because the energy in the wind increases with wind speed. Since the wind speed will vary between low wind speeds and high wind speeds, the performance criteria will change significantly during operation. In the sequel, we shall demonstrate that a systematic approach to obtain the above objectives can be achieved by the virtue of an LPV controller design. In this manner we obtain a smooth transition between controllers satisfying the design requirements along the design trajectory. Further, it shall be noted that nonlinearities caused, for example, by the aerodynamics can easily be incorporated into the LPV design framework.

3. WIND TURBINE MODEL

Based on the control objectives presented in the previous section, a nonlinear model of suitable complexity will be constructed. Then in order to obtain an LPV model, the nonlinear model is linearized along the desired operating trajectory.

It has been evaluated that five components have to be modelled in order to perform a proper controller design according to the presented requirements: drive train, tower, aerodynamics, pitch system, and generator and converter system. These five components will be presented in the following sections.

3.1. Drive train

The drive train is modelled by two inertias interconnected by a spring and a damper. In this design, the dynamics of the blades will not be included, and the blade stiffness and inertia are therefore lumped into the slow-speed shaft. Friction is included in terms of linear friction coefficients on each shaft. This leads to the following formulation of the drive train model:

$$J_r\dot{\omega}_r = Q_a - B_r\omega_r - N\mu(N\omega_r - \omega_g) - NK\theta_\Delta \tag{1a}$$

$$J_g\dot{\omega}_g = -Q_g - B_g\omega_g + \mu(N\omega_r - \omega_g) + K\theta_\Delta \tag{1b}$$

$$\dot{\theta}_\Delta = N\omega_r - \omega_g \tag{1c}$$

$$Q_{sh} = \mu(N\omega_r - \omega_g) + K\theta_\Delta \tag{1d}$$

where ω_r and ω_g are the rotational speeds of, respectively, the slow- and high-speed shaft, θ_Δ is the angular difference between slow- and high-speed shaft, Q_a and Q_g are, respectively, aerodynamic torque and generator reaction torque, J_r and J_g are the two moments of inertia, B_r and B_g are the friction coefficients on the two shafts, N is the gearing ratio, K and μ are the stiffness and damping coefficients of the interconnection of the two inertias, and Q_{sh} is the torque between the two shafts.

3.2. Tower

The tower will be modelled by a mass–spring system as in (2) with p_t as the displacement of the tower top, m is the equivalent mass, B_t is the structural damping of the tower, K_t is the tower stiffness, and F_t is the thrust on the tower

$$m\ddot{p}_t = F_t - B_t\dot{p}_t - K_t p_t \tag{2}$$

DOI: 10.1002/rnc

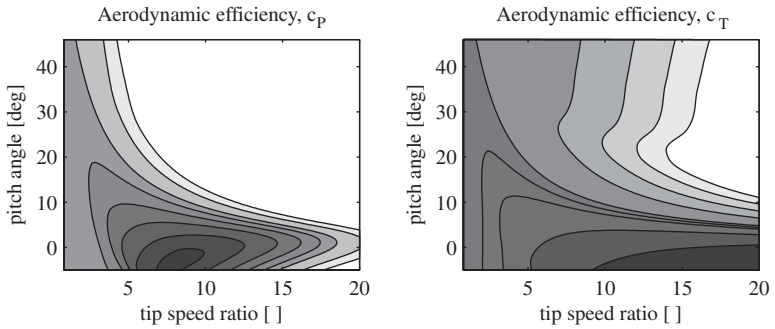

Figure 2. Illustration of aerodynamic efficiency and thrust coefficient. Light shades indicate small coefficients and dark shades indicate large coefficients.

3.3. Aerodynamics

The aerodynamics will be approximated by static functions of spatial average of wind speed, rotor speed, and pitch angle according to [17]

$$Q_{\mathrm{a}} = \frac{1}{2}\rho\pi R^2 \frac{v^3}{\omega_{\mathrm{r}}} c_P(\lambda, \beta) \tag{3a}$$

$$F_{\mathrm{t}} = \tfrac{1}{2}\rho\pi R^2 v^2 c_T(\lambda, \beta) \tag{3b}$$

$$\lambda = \frac{\omega_{\mathrm{r}} R}{v} \tag{3c}$$

where ρ is the air density, R is the rotor radius, β is the pitch angle, and λ is denoted as the tip speed ratio. The two coefficients, c_P and c_T, represent, respectively, the aerodynamic efficiency and the thrust coefficient. Figure 2 illustrates the evolution of these coefficients *versus* λ and β.

For the linearized model, the partial derivatives of the two nonlinear functions are evaluated along the desired trajectory to obtain a description of the form (4) with the tilde indicating deviations from the design equilibrium point, EQ,

$$\tilde{Q}_{\mathrm{a}} = \left.\frac{\partial Q_{\mathrm{a}}}{\partial v}\right|_{\mathrm{EQ}} \cdot \tilde{v} + \left.\frac{\partial Q_{\mathrm{a}}}{\partial \beta}\right|_{\mathrm{EQ}} \cdot \tilde{\beta} + \left.\frac{\partial Q_{\mathrm{a}}}{\partial \omega_{\mathrm{r}}}\right|_{\mathrm{EQ}} \cdot \tilde{\omega}_{\mathrm{r}} \tag{4a}$$

$$\tilde{F}_{\mathrm{t}} = \left.\frac{\partial F_{\mathrm{t}}}{\partial v}\right|_{\mathrm{EQ}} \cdot \tilde{v} + \left.\frac{\partial F_{\mathrm{t}}}{\partial \beta}\right|_{\mathrm{EQ}} \cdot \tilde{\beta} + \left.\frac{\partial F_{\mathrm{t}}}{\partial \omega_{\mathrm{r}}}\right|_{\mathrm{EQ}} \cdot \tilde{\omega}_{\mathrm{r}} \tag{4b}$$

3.4. Pitch system

The pitch system is a complicated and highly nonlinear hydraulic actuator, which on the basis of a given control voltage moves the piston and thereby rotates the blade at a certain rotational rate. To simplify the LPV controller design, an inner control loop has been designed to handle the nonlinear effects. Then the closed-loop pitch system can be described by a second-order linear model from pitch reference to pitch position. The model is presented in (5), where T_β represents the hydraulic lag and K_β represents the valve gain, pitch geometry, and controller gain. The controller gain has

DOI: 10.1002/rnc

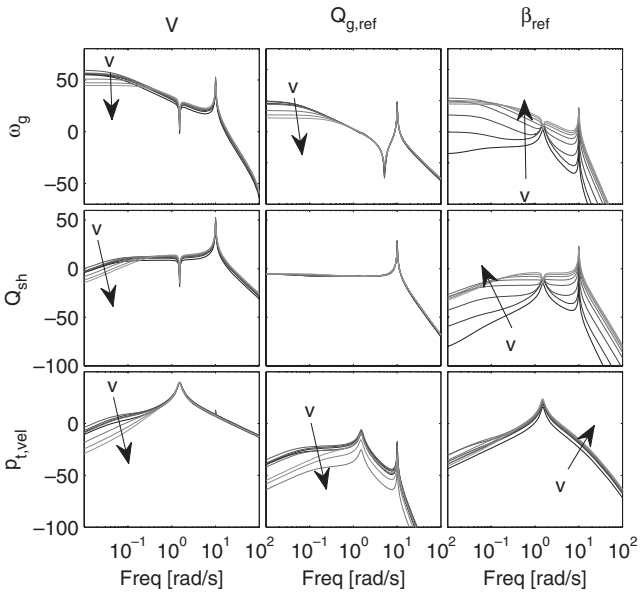

Figure 3. Magnitude plot of wind turbine model. Dark shades represent low wind speeds and light shades represent high wind speeds.

been adjusted so that the loop has a smooth response without overshoot

$$\beta(s) = \frac{K_\beta}{s(T_\beta s + 1) + K_\beta} \cdot \beta_{\text{ref}} \tag{5}$$

An interesting observation with such a servo is that it is designed to handle also extreme operating conditions such as emergency shutdown, large wind gusts, loss in grid connection, etc. This means that rate limits are not considered important during nominal operation. Here the key issue is the damage rate on, for example, blade bearings.

3.5. Generator and converter system

The dynamics of the generator and converter system are much faster than what is considered in this controller design. As a consequence, the generator and converter system is modelled by a static gain. However, an inner controller is included in order to produce the power demand from the outer controller and to smoothen out power fluctuations. When interconnecting this inner controller with the generator and converter system, the loop can be represented by a first-order filter of the form (6) in which P_e is the active power, $Q_{g,\text{ref}}$ is a torque reference, and T_0 is the constant part of the time constant (6).[‡] Note that it is already on a very simple LPV form, i.e. affine dependency

$$Q_g = \frac{T_0 \omega_g}{s + T_0 \omega_g} Q_{g,\text{ref}}, \quad P_e = \eta Q_g \omega_g \tag{6}$$

[‡]The authors are aware of the abuse of notation since ω_g varies in time.

DOI: 10.1002/rnc

3.6. Interconnection

With the above-described components, the wind turbine model can be obtained by the standard interconnection of the blocks described in the above sections. The only nonlinear components described above are the aerodynamics and generator system. With the assumption that the wind turbine is operating on the nominal trajectory specified in Figure 1, the equilibrium values for pitch angle and rotor/generator speed can be described uniquely by the wind speed. This means that the wind turbine model can be described by an LPV model scheduled on only wind speed as illustrated in Figure 3.

4. CONTROLLER STRUCTURE

Before discussing the specific choice of the controller structure, it is important to understand the desired behaviour of the control system in the different operating modes. In partial load operation, an important objective is to maximize the electrical power production. This means that the pitch angle and rotor speed should be controlled in a way so that the aerodynamic coefficient, c_P, is maximized. By observing the leftmost illustration in Figure 2, it implies that the pitch angle should be kept constant close to -2° and the rotor speed should be controlled proportional to the effective wind speed to get an optimal tip speed ratio. In practice, this will be done by tracking a generator speed reference via an update of the generator torque.

In full load operation, the generator speed and power needs to be kept close to constant nominal values, which means that the generator torque should be varied as little as possible. The pitch position as the remaining control signal is controlled to keep the aerodynamic power constant thereby keeping the electric power constant.

The main part of the controller structure is then a set-up for tracking a specified generator speed reference by mainly using generator torque in partial load operation and pitch angle in full load operation. On top of this main structure, there will be components using both control signals in order to minimize the oscillations in drive train and tower fore–aft movement. For the minimization of tower oscillations a measurement of tower acceleration is included.

When designing linear controllers for a nonlinear system, the system is typically linearized by using a first-order Taylor series of the nonlinear differential equation. When doing this, the equilibrium is subtracted from the model variables resulting in a model which, in the new set of variables, has its equilibrium in the origin. Then when implementing the controller in practice, the control signals associated with the equilibrium in the design must be added to the output of the controller. Similarly, the equilibrium point value of the measurements should be subtracted from the online measurements. In this controller formulation, the LPV model will be obtained using linearization along a chosen operating trajectory. This means that the same issue therefore applies to the implementation of the controller, which is illustrated in Figure 4. In the block diagram the three blocks having inputs from estimated wind speed, $\hat{v}$, should be interpreted as nonlinear static functions of an estimate of the effective wind speed—derived from the equilibrium conditions described in Figure 1. The wind speed estimate can for this purpose be calculated using a dynamic observer as in [18].

From Figure 4 it can be seen that this way of handling the issue of equilibrium points being different from the origin will lead to feed-forward terms. For classical controllers such feed-forward terms have proven to be beneficial as discussed in the Introduction. There is, however, a risk that the feed-forward term might degrade overall performance if it operates in the same frequency region

DOI: 10.1002/rnc

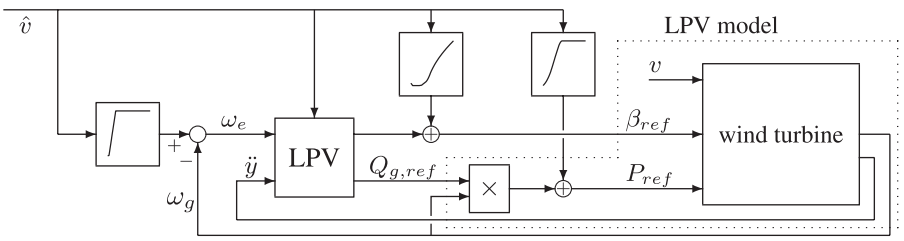

Figure 4. Implementation structure for an LPV controller based on linearization along a trajectory of equilibrium points.

as the LPV controller. In this case it should be included in the LPV design using a two degrees-of-freedom controller design, e.g. along the lines of [19]. It is expected that the feed-forward terms will not interfere with the LPV controller because of the successful results obtained for classical controllers. The LPV design presented in this paper will, therefore, not include feed-forward terms, because this would increase the dimensionality of the design problem and thereby make numerical difficulties more likely.

5. SELECTION OF PERFORMANCE CHANNELS AND ASSOCIATED WEIGHTS

In the applied formulation of LPV control, the performance is measured in terms of energy amplification from a number of selected inputs to a selection of outputs—very similar to $\mathscr{H}_\infty$ control. However, the objectives in Section 2 are given in physical terms, such as to minimize the fatigue damage in the tower, to limit the maximum generator speed, etc. As performance input, the wind speed is chosen and to transform the objectives into something that can be measured by energy amplification, the following performance outputs have been chosen.

Tower top velocity in the fore–aft direction, $\dot{y}$: The tower is lightly damped close to its eigen-frequency and it is therefore most important to actively dampen oscillations around this frequency. In the linearized model, the bode diagram of the transfer function from wind speed to tower top velocity has a peak at the tower eigenfrequency—along the entire operating trajectory. Thus, by introducing a frequency-independent scaling of this performance output, the dampening of the oscillations around the tower eigenfrequency can be included in the performance function for controller design.

Torsion torque in drive train, Q_{sh}: For the drive train the issue is very similar, because it is lightly damped around its eigenfrequency. The bode diagram of the transfer function from wind speed to shaft torque has a peak at this eigenfrequency, which means that a frequency-independent scaling can be used—with the same argumentation as for the tower.

Tracking error for generator speed, ω_{e}: The main target of using this performance output is to minimize the variations in generator speed, from the design trajectory, caused by variations in wind speed. The main content of the wind speed is in lower frequencies, which means that putting an emphasis on low-frequency components will be satisfactory. Because the low-frequency components are dominant in the transfer function from wind speed to generator speed (for all the linearized models) this means that again a frequency-independent scaling is applicable. However, the scaling should be gain scheduled by effective wind speed to take into account that the issue of

DOI: 10.1002/rnc

overspeeds is most likely to occur around rated generator speed, i.e. a larger weight for medium wind speeds than on high and low wind speeds should be used.

Pitch activity, β: It is very undesirable to have high-frequency content in the controlled pitch angle because this would cause a high amount of wear in blade bearings and in the pitch hydraulics. In partial load operation, there is a very limited control authority in the pitch actuator because the wind turbine is operating close to aerodynamic optimality. As a consequence, the generator torque is the main control signal in low wind speeds and it is cheap to limit pitch activity in this region. At high wind speeds, the pitch system is the main actuator and limiting the pitch activity has a much higher impact on the other structural loads. It has therefore been decided to gain schedule the weight on pitch activity to allow for high activity in full load operation and low activity in partial load operation. Further, the weight will be in the form of a high pass filter to make the high-frequency pitch activity more expensive than the low-frequency activity.

Variations in generator torque, Q_g: In the linearized model for controller design, the electrical power is not directly accessible as a linear combination of states and inputs. In full load operation, where the steady-state generator speed is constant, the variations in generator torque relate in a direct way to power fluctuations. Therefore, the generator torque will be weighted by a large frequency-independent scaling at high wind speeds, whereas a smaller scaling is used for low wind speeds to allow for sufficient tracking of generator speed reference.

With the selected performance inputs, outputs, and weighting functions, the open-loop model for the LPV design can now be formulated with the inputs and outputs defined in (7), where u is the control signal, y represent measured outputs, and w and z represent performance inputs/outputs. The gain-scheduled parameters of these performance weights are illustrated in Figure 5

$$z = \begin{bmatrix} W_{\dot{y}}(\hat{v}) & 0 & 0 & 0 & 0 \\ 0 & W_{Q_{\mathrm{sh}}}(\hat{v}) & 0 & 0 & 0 \\ 0 & 0 & W_{\omega}(\hat{v}) & 0 & 0 \\ 0 & 0 & 0 & W_{\beta}(\hat{v}) \cdot \dfrac{(0.6 \cdot s+1)^3}{(10^{-3} \cdot s+1)^3} & 0 \\ 0 & 0 & 0 & 0 & W_{Q_{\mathrm{g}}}(\hat{v}) \end{bmatrix} \begin{bmatrix} \dot{p}_{\mathrm{t}} \\ Q_{\mathrm{sh}} \\ \omega_{\mathrm{e}} \\ \beta \\ Q_{\mathrm{g}} \end{bmatrix} \tag{7a}$$

$$w = v, \quad y = \begin{bmatrix} \omega_{\mathrm{e}} \\ \ddot{p}_{\mathrm{t}} \end{bmatrix}, \quad u = \begin{bmatrix} \beta_{\mathrm{ref}} \\ Q_{\mathrm{g,ref}} \end{bmatrix} \tag{7b}$$

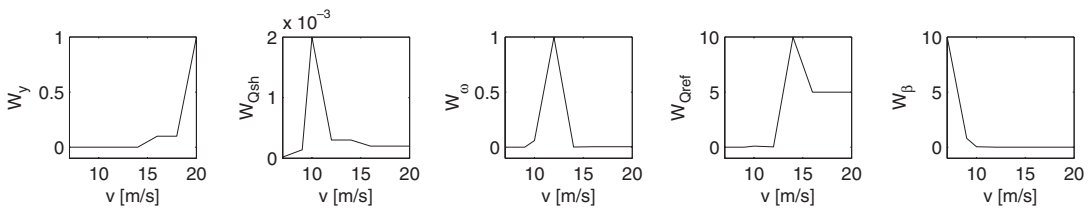

Figure 5. Illustration of parameter variation of performance weights.

DOI: 10.1002/rnc

It is expected that the control law will result in a high amount of $3P$[§] content. These oscillations originate from the varying air flow on the blades, e.g. due to a blade passing the tower. Dampening these oscillations will require a large amount of pitch activity and it is estimated that the cost in terms of wear in blade bearings is much higher than the gain in dampening of $3P$ oscillations. As a consequence, a notch filter will be applied to the control outputs at the $3P$ frequency. Because the $3P$ frequency is close to the drive train eigenfrequency, an oscillator is also applied to the control signal, $Q_{\mathrm{g,ref}}$, by using the ideas from internal model control.

6. LINEAR PARAMETER VARYING CONTROL

With the overall controller structure presented in Section 4, the control objectives given in Section 2, and the choice of performance channels and weights decided in Section 5, the preparations for the dynamic LPV controller design have been done. This leads to the design of an LPV controller for the control of wind turbines. This section will present the base of the algorithm for controller synthesis and construction.

6.1. Synthesis of LPV controllers

In [20] an analysis is provided for LPV closed-loop systems under the assumption of slowly varying parameters and in [21, 22] the general framework for designing LPV controllers with arbitrary rate of variation was presented in a linear matrix inequality (LMI) formulation. In the following, the design procedure is summarized and it is discussed how to handle numerical difficulties that might occur for higher-order systems.

During this section, an abstract representation will be used for the model derived in Section 3 combined with the performance weights. We consider a weighted open-loop model of the form (8a), which is created along standard lines for system interconnection as done in [23]. We will then search for a controller, (8b), of similar structure as the open-loop model to satisfy a specified closed-loop performance. The model and controller can be interconnected to a closed-loop representation described by short-hand notation in (8c), for which it can be observed that the formulation is affine in the controller variables

$$\begin{bmatrix} \dot{x}(t) \\ z(t) \\ y(t) \end{bmatrix} = \begin{bmatrix} A(\delta(t)) & B_p(\delta(t)) & B(\delta(t)) \\ C_p(\delta(t)) & D(\delta(t)) & E(\delta(t)) \\ C(\delta(t)) & F(\delta(t)) & 0 \end{bmatrix} \begin{bmatrix} x(t) \\ w(t) \\ u(t) \end{bmatrix} \tag{8a}$$

$$\begin{bmatrix} \dot{x}_{\mathrm{c}}(t) \\ u(t) \end{bmatrix} = \begin{bmatrix} A_{\mathrm{c}}(\delta(t)) & B_{\mathrm{c}}(\delta(t)) \\ C_{\mathrm{c}}(\delta(t)) & D_{\mathrm{c}}(\delta(t)) \end{bmatrix} \begin{bmatrix} x_{\mathrm{c}}(t) \\ y(t) \end{bmatrix} \tag{8b}$$

$$\begin{bmatrix} \dot{x}_{\mathrm{cl}}(t) \\ z(t) \end{bmatrix} = \begin{bmatrix} A_{\mathrm{cl}}(\delta(t)) & B_{\mathrm{cl}}(\delta(t)) \\ C_{\mathrm{cl}}(\delta(t)) & D_{\mathrm{cl}}(\delta(t)) \end{bmatrix} \begin{bmatrix} x_{\mathrm{cl}}(t) \\ w(t) \end{bmatrix} \tag{8c}$$

[§] The $3P$ frequency is three times the rotational speed of the rotor.

DOI: 10.1002/rnc

In the above equations, $x(t)$ and $x_c(t)$ denote the state vector of, respectively, the open-loop system and controller, $y(t)$ is the measured variables, and $u(t)$ is a vector of control signals. The input from the performance channel is denoted by $w(t)$ and its associated output is $z(t)$. It can be noted that all system and controller matrices depend on a time-varying parameter, $\delta(t)$, which is assumed to be online available (not necessarily a measured variable—it could also be the output from an estimator) and therefore also used to schedule the controller.

Throughout this paper we will use the induced $\mathscr{L}_2/\mathscr{L}_2$ gain as a performance measure, which essentially measures the energy amplification through a specified performance channel. For a closed-loop system described by (8c) we state that it satisfies a performance level γ if (9) is satisfied for all trajectories of the system in which the inputs are non-zero and have finite energy

$$\int_0^\infty z(t)^{\mathrm{T}} z(t)\,\mathrm{d}t < \gamma^2 \int_0^\infty w(t)^{\mathrm{T}} w(t)\,\mathrm{d}t \tag{9}$$

It has been shown in [24, 25] that an LPV controller can be determined through convex optimization to satisfy a closed-loop performance level, γ. To determine if a controller exists for a given performance level we can use Theorem 1.

Theorem 1

Consider an open-loop system described by (8a) with an associated parameter, $\delta(t) \in \Delta$, allowed to vary arbitrarily fast. Then there is a stabilizing controller of the form (8b) that satisfies a closed-loop performance level, γ, if there exist symmetric matrices X and Y satisfying (10) for all possible parameter values, $\delta \in \Delta$, with an arbitrary rate of variation

$$\begin{bmatrix} X & I \\ I & Y \end{bmatrix} \succ 0 \tag{10a}$$

$$\begin{bmatrix} C(\delta)_\perp \\ F(\delta)_\perp \end{bmatrix}^{\mathrm{T}} \begin{bmatrix} I & 0 \\ 0 & I \\ A(\delta) & B_p(\delta) \\ C_p(\delta) & D(\delta) \end{bmatrix}^{\mathrm{T}} \begin{bmatrix} 0 & 0 & X & 0 \\ 0 & -\gamma I & 0 & 0 \\ X & 0 & 0 & 0 \\ 0 & 0 & 0 & \dfrac{1}{\gamma} I \end{bmatrix} \begin{bmatrix} I & 0 \\ 0 & I \\ A(\delta) & B_p(\delta) \\ C_p(\delta) & D(\delta) \end{bmatrix} \begin{bmatrix} C(\delta)_\perp \\ F(\delta)_\perp \end{bmatrix} \prec 0 \tag{10b}$$

$$\begin{bmatrix} B(\delta)_\perp^{\mathrm{T}} \\ E(\delta)_\perp^{\mathrm{T}} \end{bmatrix}^{\mathrm{T}} \begin{bmatrix} -A(\delta)^{\mathrm{T}} & -C_p(\delta)^{\mathrm{T}} \\ -B_p(\delta)^{\mathrm{T}} & -D(\delta)^{\mathrm{T}} \\ I & 0 \\ 0 & I \end{bmatrix}^{\mathrm{T}} \begin{bmatrix} 0 & 0 & Y & 0 \\ 0 & -\dfrac{1}{\gamma} I & 0 & 0 \\ Y & 0 & 0 & 0 \\ 0 & 0 & 0 & \gamma I \end{bmatrix}$$

$$\times \begin{bmatrix} -A(\delta)^{\mathrm{T}} & -C_p(\delta)^{\mathrm{T}} \\ -B_p(\delta)^{\mathrm{T}} & -D(\delta)^{\mathrm{T}} \\ I & 0 \\ 0 & I \end{bmatrix} \begin{bmatrix} B(\delta)_\perp^{\mathrm{T}} \\ E(\delta)_\perp^{\mathrm{T}} \end{bmatrix} \succ 0 \tag{10c}$$

DOI: 10.1002/rnc

The matrix inequalities in Theorem 1 are clearly affine in the variables X and Y. In the context of controller synthesis, it is typically desirable to determine a controller that minimizes γ and not only one that satisfies a pre-specified performance specification. This can be done by bisection or alternatively by using the well-known Schur lemma, whereby the two matrix inequalities are transformed into matrix inequalities that are also linear in γ. Then γ can be used directly in the optimization problem.

In the above performance specification, it is required to solve infinitely many LMIs—one for each possible parameter—and the problem cannot therefore be solved in finite time. In the special case of affine parameter dependency and with the parameters varying within a convex polytope, the problem reduces to checking only the vertices [26]. As discussed in the Introduction, affine parameter dependency is not expected to give a satisfactory performance for the application in mind. Alternatively, a method has been developed for designing controllers for the case of rational parameter dependency [27, 28]. This approach is much more appealing, but suffers from numerical issues in the construction of controllers from the synthesis variables. One issue is that the numerics are highly dependent on the choice (and size) of a linear fractional representation, which makes it a very demanding task to design controllers for which the performance function is scheduled, and the scheduling might change between iterations in the design process. Because of these reasons, it has been chosen to focus on an approximative method (using a grid) presented in [29] but still with the assumption of arbitrarily fast parameter variations.

The density of the grid is to be determined from a trade-off between having a lot of grid points causing heavy computational time and a few grid points not catching the nonlinear behaviour to a sufficient degree. It can be shown that if a parameterized LMI is satisfied for two selected parameter values, the parameterized LMI will also be satisfied for a convex combination of the two parameters—see, for example [23]. This means that if we can assume affine parameter dependency of the weighted open loop in the interval between two grid points, the stability and performance will be given for the intermediate parameter values. For the specific application of LPV control for wind turbines, it has been chosen to select two grid points in each of the following three operating modes: partial load operation with variable generator speed, partial load operation with nominal generator speed, and full load operation. This provides an acceptable trade-off between having a few number of grid points and not violating the assumption of piecewise affine parameter dependency too much.

6.2. Controller construction

By solving the optimization problem for controller synthesis in Theorem 1, we get an achievable performance level, γ, and the matrices X and Y for the quadratic storage/Lyapunov function used to measure the performance and stability of the closed-loop interconnection.

Note that the controller variables A_c, B_c, C_c, and D_c are not directly available from Theorem 1. Fortunately, a method for constructing the controller variables has been developed in which an LMI containing the controller variables can be constructed and solved analytically from the result of (10).

The details can be found in [24, 25] and in this paper we focus only on the actual procedure for constructing the controller when X and Y have been determined. To simplify the notation, we rewrite (10b) and (10c) as in (11) with the variables defined in (12)

$$R_{\perp}^{\mathrm{T}} \begin{bmatrix} I \\ Q \end{bmatrix}^{\mathrm{T}} P \begin{bmatrix} I \\ Q \end{bmatrix} R_{\perp} \prec 0 \tag{11a}$$

DOI: 10.1002/rnc

$$L_\perp^{\mathrm{T}} \begin{bmatrix} -Q^{\mathrm{T}} \\ I \end{bmatrix}^{\mathrm{T}} P^{-1} \begin{bmatrix} -Q^{\mathrm{T}} \\ I \end{bmatrix} L_\perp \succ 0 \tag{11b}$$

$$L = \begin{bmatrix} 0 & B(\delta) \\ I & 0 \\ 0 & E(\delta) \end{bmatrix}^{\mathrm{T}}, \quad R = \begin{bmatrix} 0 & I & 0 \\ C(\delta) & 0 & F(\delta) \end{bmatrix}, \quad Q = \begin{bmatrix} A(\delta) & 0 & B_p(\delta) \\ 0 & 0 & 0 \\ C_p(\delta) & 0 & D(\delta) \end{bmatrix} \tag{12a}$$

$$P = \begin{bmatrix} 0 & 0 & X_{\mathrm{cl}} & 0 \\ 0 & -\gamma I & 0 & 0 \\ X_{\mathrm{cl}} & 0 & 0 & 0 \\ 0 & 0 & 0 & \dfrac{1}{\gamma} I \end{bmatrix}, \quad X_{\mathrm{cl}} = \begin{bmatrix} X & U \\ U^{\mathrm{T}} & \hat{X} \end{bmatrix}, \quad X_{\mathrm{cl}}^{-1} = \begin{bmatrix} Y & V \\ V^{\mathrm{T}} & \hat{Y} \end{bmatrix} \tag{12b}$$

The observant reader would have noticed that all variables in (12) are available except for the variables in X_{cl}. For this variable, only X and Y are directly available. In [30] it is suggested to calculate as in (13). Construction of the state-space controller in (8b) can then be described in Algorithm 2

$$X_{\mathrm{cl}} = \begin{bmatrix} Y & V \\ I & 0 \end{bmatrix}^{-1} \begin{bmatrix} I & 0 \\ X & U \end{bmatrix}, \quad UV^{\mathrm{T}} = I - XY \tag{13}$$

Algorithm 2

Step 1: Choose non-singular matrices Φ and Ψ such that $L\Phi = [L_1 \; 0]$ and $R\Psi = [R_1 \; 0]$ so that $L_1 \in \mathbb{R}^{n_L \times m_L}$ and $R_1 \in \mathbb{R}^{n_R \times m_R}$ have a full column rank.

Step 2: Let

$$\Lambda = \begin{bmatrix} \Lambda_{11} & \Lambda_{12} \\ \Lambda_{21} & \Lambda_{22} \end{bmatrix} \triangleq \Phi^{\mathrm{T}} Q \Psi, \quad \Upsilon \triangleq \begin{bmatrix} I & 0 \\ 0 & 0 \\ 0 & I \\ \Lambda_{21} & 0 \end{bmatrix}, \quad \Omega \triangleq \begin{bmatrix} 0 \\ I \\ \Lambda_{12} \\ \Lambda_{22} \end{bmatrix}$$

$$\Pi \triangleq \begin{bmatrix} \Psi & 0 \\ 0 & \Phi^{-\mathrm{T}} \end{bmatrix}^{\mathrm{T}} P \begin{bmatrix} \Psi & 0 \\ 0 & \Phi^{-\mathrm{T}} \end{bmatrix}$$

Step 3: Find $\Theta_1 \in \mathbb{R}^{m_L \times m_R}$ and Θ_2 such that

$$\begin{bmatrix} \Theta_1 \\ \Theta_2 \end{bmatrix}^{\mathrm{T}} (\Upsilon^{\mathrm{T}} \Pi \Upsilon - \Upsilon^{\mathrm{T}} \Pi \Omega (\Omega^{\mathrm{T}} \Pi \Omega)^{-1} \Omega^{\mathrm{T}} \Pi \Upsilon) \begin{bmatrix} \Theta_1 \\ \Theta_2 \end{bmatrix} \prec 0 \tag{14}$$

e.g. by an eigenvalue decomposition.

DOI: 10.1002/rnc

Step 4: Then

$$\begin{bmatrix} A_c(\delta) & B_c(\delta) \\ C_c(\delta) & D_c(\delta) \end{bmatrix} = L_1^{-T}(\Theta_2\Theta_1^{-1} - \Lambda_{11})R_1^{-1}$$

7. NUMERICAL CONDITIONING OF AN LPV CONTROLLER DESIGN

To summarize we have seen that the LPV controller design problem can be solved by determining X and Y satisfying (10) for which γ is minimized. Then X_{cl} can be constructed using (13), and the controller matrices in K can then be determined by Algorithm 2 with variables as in (12). In practice, the solution is unfortunately not that simple because numerical issues might make the controller construction impossible if no extra measures are taken. This section will present methods for conditioning the controller synthesis and construction to make it possible to design LPV controllers for practical applications.

7.1. Inversion of $\Omega^T\Pi\Omega$

It can be shown that (11a) is equivalent to requiring $\Omega^T\Pi\Omega \prec 0$. This means that $\Omega^T\Pi\Omega$ is always non-singular, but in practice it might become very ill-conditioned which can be seen from the particular set-up for control of wind turbines. In this application, the primal LMI has a condition number in the order of 10^{10} and it is concluded that the inversion of a matrix that is ill-conditioned might affect the numerical conditioning of the algorithm. In [31] a remedy is suggested by an appropriate scaling of Ψ.

Choose $\tilde{\Psi}$ such that $R\tilde{\Psi} = [\tilde{R}_1 \ 0]$ as in Algorithm 2, e.g. by a singular value decomposition of R. Then let

$$J = \begin{bmatrix} J_{11} & J_{12} \\ J_{21} & J_{22} \end{bmatrix} = \tilde{\Psi}^T \begin{bmatrix} I \\ Q \end{bmatrix}^T P \begin{bmatrix} I \\ Q \end{bmatrix} \tilde{\Psi}, \quad \Psi = \tilde{\Psi} \begin{bmatrix} I & 0 \\ 0 & Q \end{bmatrix}, \quad Q^T Q = -J_{22}^{-1}$$

We can observe that Ψ satisfies the condition $R\Psi = [R_1 \ 0]$, now with $\Omega^T\Pi\Omega \approx -I$. We are of course still left with finding a suitable Q, which is not easier from a numerical point of view, but the point is that even with an approximate solution $\Omega^T\Pi\Omega$ is made better conditioned.

7.2. Conditioning of variables

The main matrix inequality used to determine the controller variables is (14), which contains a number of products between matrices, Υ, Π, and Ω. If one or more of these variables are ill-conditioned, numerical errors might make small negative eigenvalues of (14) shift to positive eigenvalues, which in the end means that it is impossible to determine Θ_1 and Θ_2 of appropriate dimension that renders the matrix inequality satisfied.

The conditioning of Υ and Ω is given mainly by the norm of Q and Ψ, because they are bounded from below by 1. If a proper realization is chosen (e.g. according to the discussion above and by scaling of the inputs and outputs), the norm of Q will not have any significant impact on the numerical stability of the algorithm. The norm of Ψ will be given mainly by the square root of J_{22}, which is expected to have a norm in the same scale as P. This means that with a proper choice of

DOI: 10.1002/rnc

realization and scaling of inputs and outputs, the numerical issues in controller construction with the proposed algorithm is determined by the conditioning of Π and thereby P.

For reasonable choices of performance level (γ close to 1), the conditioning of P is given by the conditioning of X_{cl}. X_{cl} is unfortunately often close to being singular when the optimization problem approaches optimum. A remedy is to take advantage of the partitioning used for constructing X_{cl}. In [23], four different modifications to (11) have been investigated and it has been found promising to modify the variables for the construction algorithm in order to distribute the conditioning more evenly. This can be done by performing the variable substitution in (15)

$$P_{\mathrm{new}}=\begin{bmatrix} 0 & 0 & X_1^{-1} & 0 \\ 0 & -\gamma I & 0 & 0 \\ X_1^{-\mathrm{T}} & 0 & 0 & 0 \\ 0 & 0 & 0 & \dfrac{1}{\gamma} I \end{bmatrix}, \quad Q_{\mathrm{new}}=\begin{bmatrix} X_2 & 0 \\ 0 & I \end{bmatrix} Q, \quad L_{\mathrm{new}}=L\begin{bmatrix} X_2^{\mathrm{T}} & 0 \\ 0 & I \end{bmatrix} \tag{15}$$

We now need to choose X_1 and X_2 appropriately in order to optimize numerical performance. Three different approaches have been investigated in [23] and it has been found that method presented in the following has superior performance.

We will take advantage of the requirement of X and Y being symmetric and positive definite. This means that they can be expressed as $X=M^{\mathrm{T}}M$ and $Y=N^{\mathrm{T}}N$, e.g. by a Cholesky factorization. Then (13) can be rearranged as (16)

$$X_{\mathrm{cl}}=\begin{bmatrix} N^{\mathrm{T}}N & V \\ I & 0 \end{bmatrix}^{-1}\begin{bmatrix} I & 0 \\ M^{\mathrm{T}}M & U \end{bmatrix}=\begin{bmatrix} N & N^{-\mathrm{T}}V \\ M^{-\mathrm{T}} & 0 \end{bmatrix}^{-1}\begin{bmatrix} N^{-\mathrm{T}} & 0 \\ M & M^{-\mathrm{T}}U \end{bmatrix} \tag{16}$$

If we denote

$$ST^{\mathrm{T}}=M^{-\mathrm{T}}UV^{\mathrm{T}}N^{-1}=M^{-\mathrm{T}}N^{-1}-MN^{\mathrm{T}} \tag{17}$$

we can describe X_1 and X_2 in the following equation:

$$X_1=\begin{bmatrix} N & T \\ M^{-\mathrm{T}} & 0 \end{bmatrix}, \quad X_2=\begin{bmatrix} N^{-\mathrm{T}} & 0 \\ M & S \end{bmatrix} \tag{18}$$

7.3. Bounding synthesis LMIs and variables

The remedies presented in Sections 7.1 and 7.2 involve modifications to the construction algorithm to render the controller construction possible from a numerical point of view. In practical applications, the controller construction might still fail because of numerical issues.

For a typical application, X and Y will become large when reaching optimum and $I-XY$ will be close to singular. This means that the construction of X_1 and X_2 of full rank is difficult because U or V (or equivalently S and T) will be ill-conditioned. In the particular application, this is also the case with $I-XY$ having a condition number in the order of 10^{13}. To handle this issue a slack variable β has been included in the coupling condition (10a) as in (19) to separate the

DOI: 10.1002/rnc

eigenvalues of X from the eigenvalues of Y^{-1}. With a Schur complement of (19) and a reordering of the terms, we can see that $I - XY \prec -(\beta^2 - 1)I$ which means that by increasing β we can make $I - XY$ better conditioned

$$\begin{bmatrix} Y & \beta I \\ \beta I & X \end{bmatrix} \succ 0 \tag{19}$$

As mentioned, X and Y might also become very large in norm which increases the norm of X_1 and X_2 and in many cases making them worse-conditioned. To avoid this an upper bound is included for the two variables.

It should be noted that these introduced coefficients and bounds come with the cost that the synthesis problem in Theorem 1 most likely will not satisfy the performance criterion, γ, with the introduced bounds. This means that it might be necessary to go for a controller satisfying a slightly poorer performance level. For the particular application, this means a decrease in performance from $\gamma = 1$ to $\gamma = 1.33$.

7.4. Design algorithm

In summary we can design a controller to satisfy a given performance specification by following Algorithm 3.

Algorithm 3

Step 1: Determine X and Y by solving the set of LMIs in Theorem 1.
Step 2: Determine a representation for X_1 and X_2 according to (18).
Step 3: Calculate the controller, K, from Algorithm 2 with the suggested modifications.
Step 4: If controller construction fails, bound critical variables/LMIs and reiterate from Step 2.

8. SIMULATION RESULTS

The proposed design algorithm has been applied to the control of wind turbines. The gain and time constant in the performance weights have been chosen by an iterative procedure by first designing a linear time invariant (LTI) controller at the operating points to satisfy the desired performance specifications after which the LPV controller is designed. This design has resulted in the controller illustrated in Figure 6 in which the most noticeable observation is the switch between mainly using a generator torque at low wind speeds and a pitch at high wind speeds.

In the design procedure it was experienced that it was necessary to exaggerate the gain of the performance weights to get appropriate performance from a simulations point of view. Especially the weight on pitch at low wind speeds, tracking error of generator speed at mid wind speeds, and generator torque at high wind speeds needed to be modified significantly from the LTI design to the LPV design to get similar controllers. Otherwise, the LPV controller in low wind speed would resemble the high wind speed controller too much. It will be shown that the LPV controller designed using the exaggerated performance weights show satisfactory performance from simulations point of view, and the LPV controller design is therefore concluded to be successful.

DOI: 10.1002/rnc

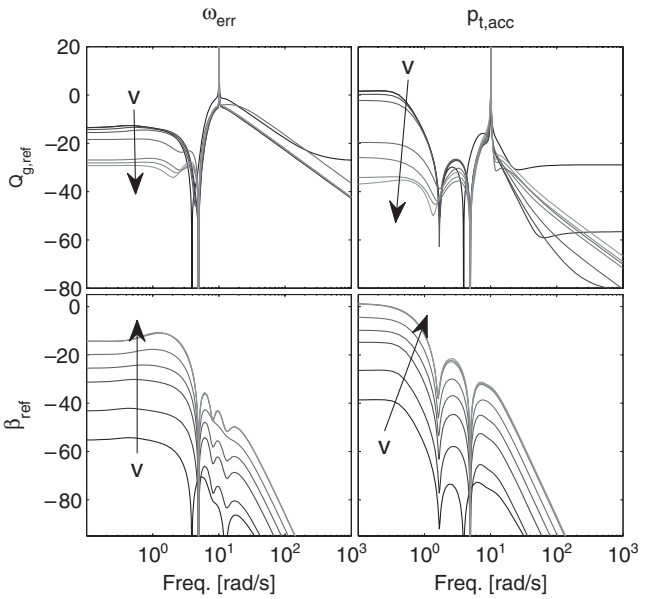

Figure 6. Magnitude plot of LPV controller. Dark shades represent low wind speeds and light shades represent high wind speeds.

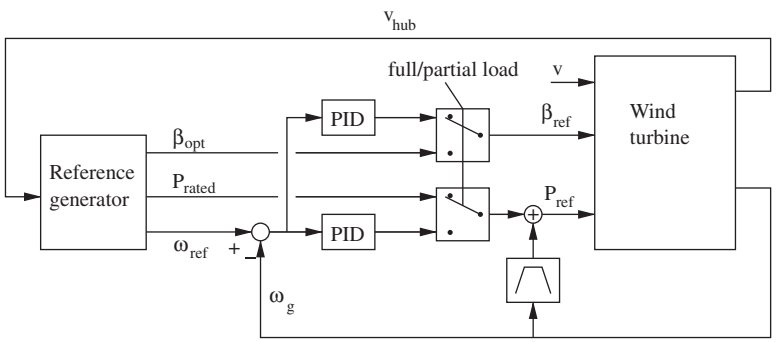

Figure 7. Block diagram of a classical controller.

8.1. Simulation set-up

A controller similar to a commercial controller has been used for simulation-based illustrations of the benefits of the designed LPV controller. In Figure 7 a rough sketch of this classical controller is presented and in what follows it will be described briefly.

The main part of the controller is a set of two proportional integral derivatives (PIDs) for tracking of generator speed. In partial load operation, one PID controller is used which has power reference as a control signal. Another PID controller is used in full load operation with pitch reference as control signal. These PID controllers are gain scheduled on the basis of generator speed and pitch

DOI: 10.1002/rnc

angle in order to take into account the variations in the aerodynamics. They have been tuned by the Ziegler–Nichols approach and are implemented with anti-windup to take into account that the control signals can be saturated. In Figure 7, a simple switching mechanism is illustrated to decide if the partial load controller or the full load controller is active. This is a simplification of the real implementation, because means have been included to allow for bumpless transfer between the two controllers. To minimize drive train oscillations, an additional loop is included which updates the power reference on the basis of generator speed variations around the drive train eigenfrequency.

The closed-loop performance has then been evaluated through simulations of both the classical controller and the LPV controller. These simulations have been performed with a stochastic wind input with turbulence according to the IEC 1A standard [32].

The performance criteria for the tracking of generator speed and active power will be measured differently in partial load and full load operations. In partial load operation, the tracking will be measured by average power production during the entire simulation. In full load operation, the tracking of power production is measured by the standard deviation on active power. For this performance criterion, time ranges are disregarded where either controller is operating in partial load. Further, in operation modes with rated generator speed, the tracking of the generator speed is measured by the difference between minimum and maximum generator speeds.

The performance for especially the fatigue damage is difficult to evaluate directly from the energy gain as discussed in [13], and the damage on tower and drive train is evaluated from rain-flow count [33]. Finally, the damage due to pitch activity is mostly on the blade bearings for which the damage can be approximated by the standard deviation of the pitch rate [33].

8.2. Partial load and variable-speed operations

A simulation result for partial load operation is shown in Figure 8 from which it can be seen that the structural movement and power production are similar for the two controllers. When observing the bottom graph it can be seen that the average power production is very similar for the two closed loops, but that the LPV controller seems to follow better the actual wind speed and thereby the energy available in the wind. It is expected that this is caused by the different means for generator reference, where the classical controller is based on hub speed measurements and the LPV controller is based on estimated wind speed. Also, a significant difference in pitch activity can be observed between the two closed loops. In Table I a comparison is given for some of the important criteria for partial load operation. Most importantly it can be seen that the damage in the blade bearing is reduced by 24% without reducing power production. Also the drive train loads are reduced by 21%. The downside is that the tower damage is increased by 12%, but this is not critical because in the low wind speeds, the absolute level in tower damage is low during low wind speeds.

8.3. Partial load and rated speed operations

In Figure 9 another simulation result is given for partial load during higher wind speeds, where the generator speed reference is saturated from above. In this operating mode you can observe a large difference in both tower movement and generator speed variation without any significant influence on average power production. Also pitch activity is reduced significantly when compared with the classical controller. A comparison of the two simulations is shown in Table II from which the most important observation is that tower loads are almost halved together with a significant decrease in

DOI: 10.1002/rnc

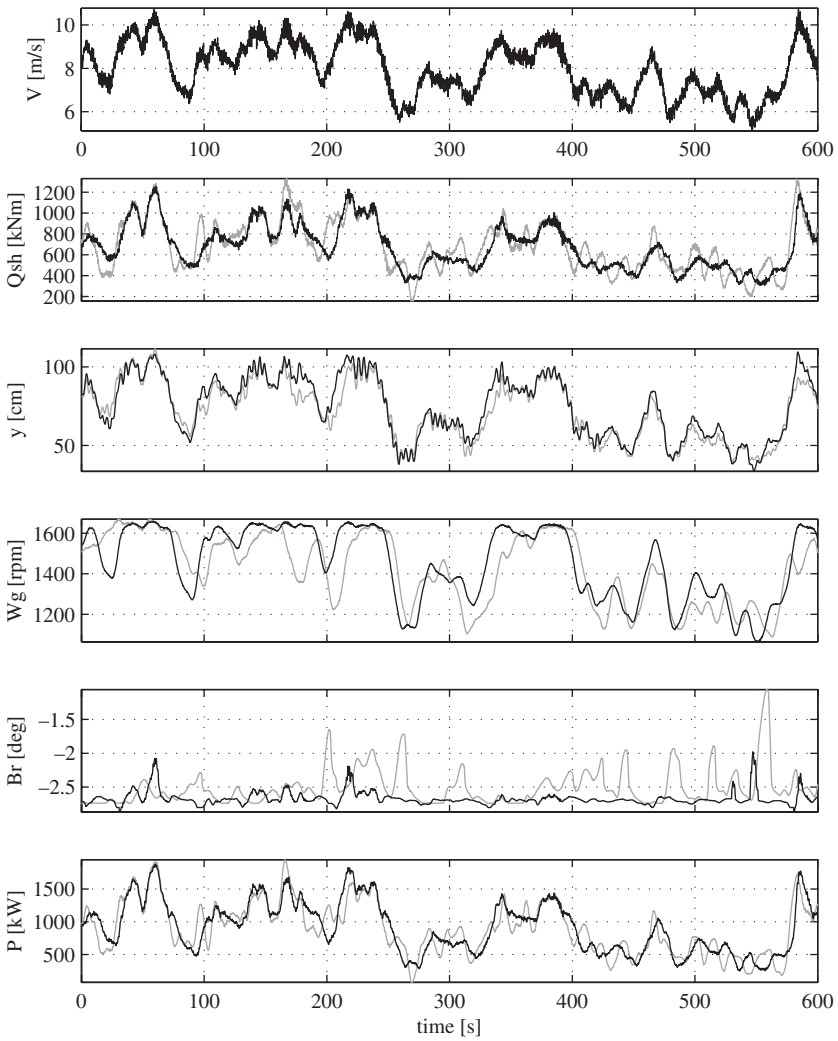

Figure 8. Simulation results for low wind speeds. Black lines: LPV controller; grey lines: classical controller. Note large difference in pitch activity.

Table I. The performance of the LPV controller is presented relative to the classical controller for the operation at low wind speeds.

	Tower damage	Drive train damage	Blade bearing damage	Average power
LPV/classic	1.12	0.79	0.76	1.01

DOI: 10.1002/rnc

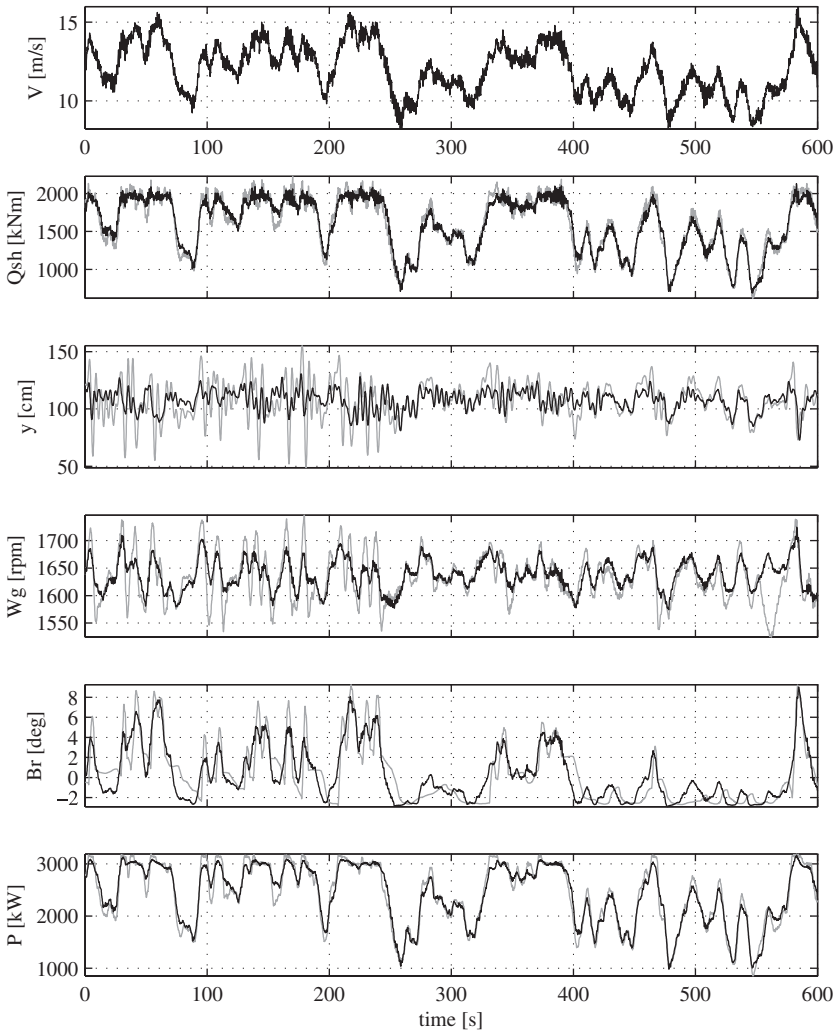

Figure 9. Simulation results for medium wind speeds. Black lines: LPV controller; grey lines: classical controller. Note large difference in tower movement and generator speed.

Table II. The performance of the LPV controller is presented relative to the classical controller for the operation at medium wind speeds.

	Tower damage	Drive train damage	Blade bearing damage	Speed peak–peak	Average power
LPV/classic	0.48	0.93	0.70	0.68	1.00

DOI: 10.1002/rnc

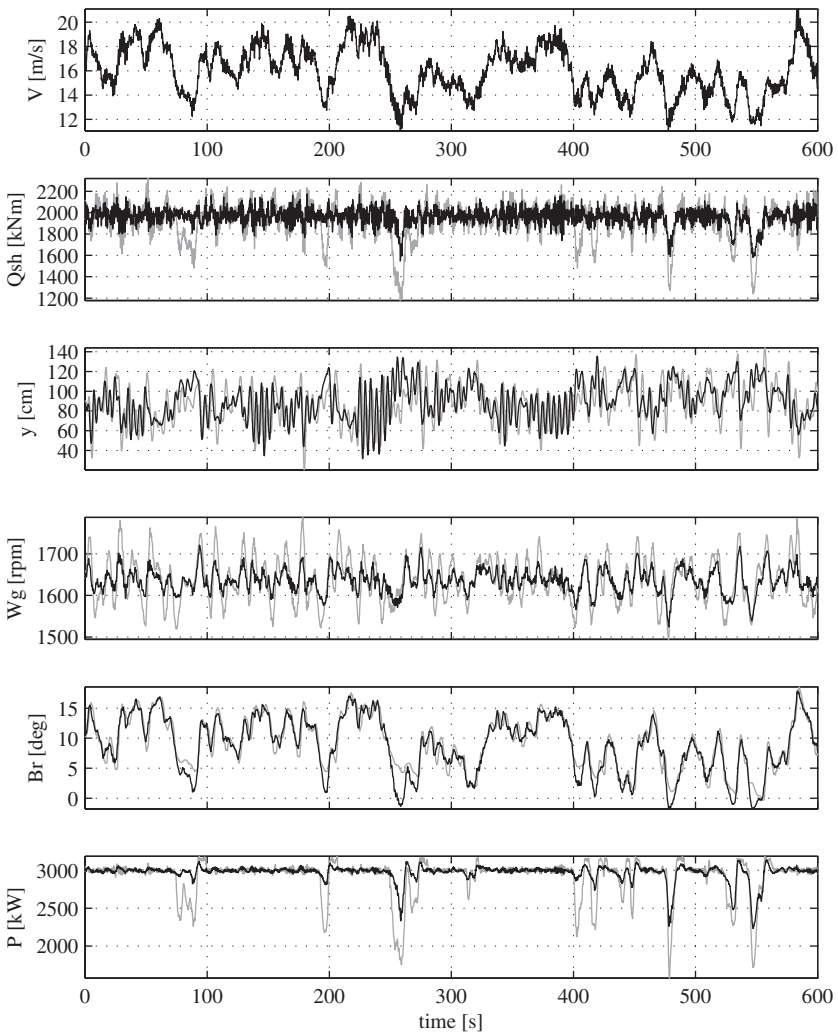

Figure 10. Simulation results for high wind speeds. Black lines: LPV controller; grey lines: classical controller.

generator speed of 32%. This is obtained without increasing the pitch activity or decreasing the average power production.

8.4. Full load operation

In full load operation, improvements can be observed when compared with the classical controller. A result from a simulation in full load is given in Figure 10 in which the most important observation is that the generator speed variations are reduced significantly without increasing structural loads. A number of power dips are also observed in the classical controller due to switching to partial load operation. The difference between the two controllers is caused by the different means for

DOI: 10.1002/rnc

Table III. The performance of the LPV controller is presented relative to the classical controller for the operation at high wind speeds.

	Tower damage	Drive train damage	Blade bearing damage	Speed peak–peak	Std. power
LPV/classic	0.85	0.56	0.98	0.67	0.94

generator references as discussed in Section 8.2. From a comparison given in Table III, it can be observed that the generator speed is reduced by 33% and drive train oscillations are reduced by 44% without increasing pitch activity, power fluctuations, or tower oscillations.

8.5. Simulation through all operating modes

Finally, the scheduling in the LPV controller is tested by performing a simulation with a wind speed varying from low wind speeds to high wind speeds. The purpose of this simulation is to investigate the controller transitions along the operating trajectory. Such a simulation is given in Figure 11 from which it can be seen that the controller provides a smooth transfer between all three operating modes: partial load control with variable generator speed reference, partial load control with fixed generator speed reference, and full load control. Also note that the tower oscillations are significantly damped when compared with the classical controller.

8.6. Summary

To summarize the three scenarios, it can be concluded that the pitch activity is decreased significantly during low wind speeds and tower and drive train loads are reduced significantly in higher wind speeds. Also the variations in generator speed are reduced in higher wind speeds—especially in full load operation with a reduction of 33%.

The performance increase comes with the only cost of higher tower loads during low wind speeds (deemed insignificant). From a design of LTI controllers at each of the three regions, it can be observed that this issue can be handled better on a local scale. When combining this with the need for exaggerating the performance weights, we get an indication that the assumption of arbitrary fast parameter variations is restrictive. It is therefore expected that an even better performance can be obtained by relaxing this constraint to rate-bounded parameter variations. This will, however, complicate the controller construction further, because X_{cl} will then be parameter dependent and the conditioning might vary significantly over wind speed. Further, there is no general method for identifying a basis function for the dependency of X_{cl} on the parameter.

9. CONCLUSIONS/DISCUSSION

This paper has presented a systematic method for designing a single control law to cover both partial load and full load operations. The proposed controller is based on the LPV design method, which can be interpreted as a gain scheduling that provides a smooth transition between different LTI controllers for a target trajectory. This enables the controller to take into account model nonlinearities and different design requirements along the operating trajectory.

The LPV design method suffers from numerical issues that make computation of the controller difficult for medium- to large-scale systems. To make the controller design with general parameter

DOI: 10.1002/rnc

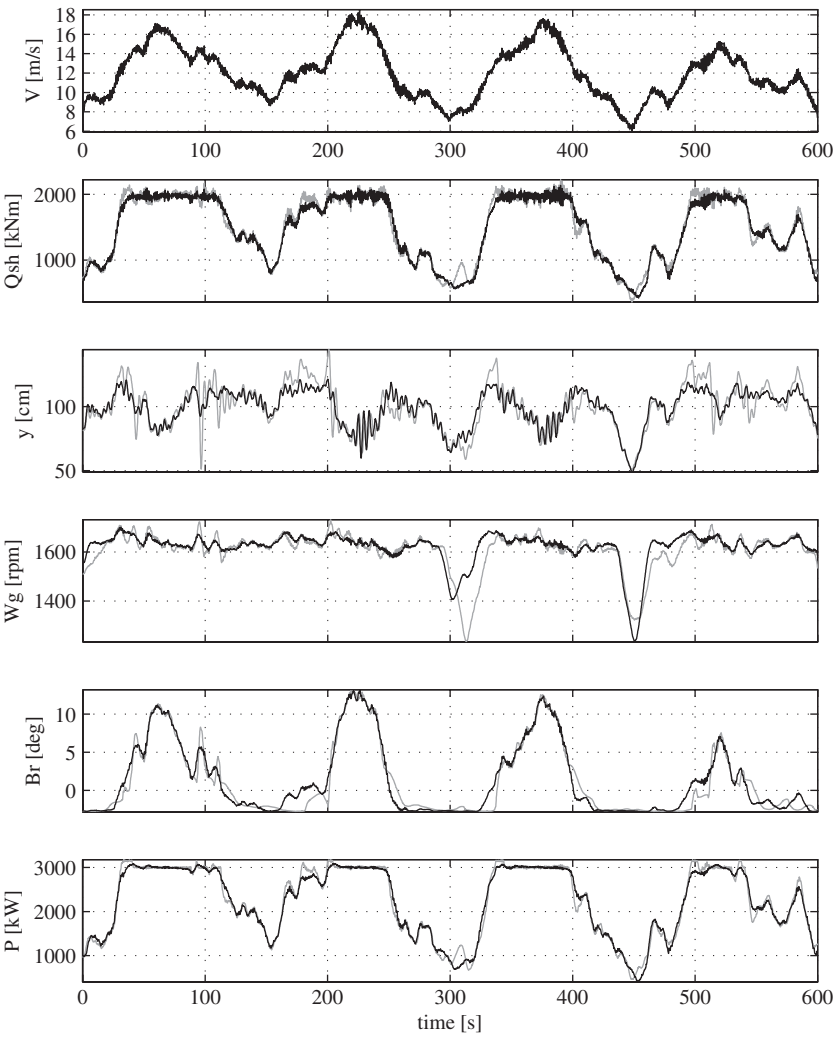

Figure 11. Simulation results for whole wind speed range. Black lines: LPV controller; grey lines: classical controller. Note smooth transition between operating modes and reduced tower oscillations.

dependency possible for the specific application, the paper has presented and discussed several issues related to the numerical computation of LPV controllers.

The proposed method for obtaining a numerically stable design algorithm has been used for the design of an LPV controller for control of wind turbines in both partial load and full load operations. Using simulation studies, the proposed controller has been compared with a controller designed using classical techniques and it has been concluded that the LPV controller achieves significantly better performance. Most importantly, a decrease in pitch activity is observed for low wind speeds and tower and drive train loads are reduced in higher wind speeds. This performance increase is obtained without affecting the produced power, power fluctuations, and generator speed

DOI: 10.1002/rnc

variations. However, the tower loads are observed to increase slightly during low wind speeds, but this increase is deemed insignificant and the design is therefore concluded to be successful.

The proposed controller has not yet been implemented on a real wind turbine. Before this can be done it should be investigated how the control law affects the structural components not included in the design model, e.g. blade dynamics and tower sideways movement.

Finally, it has been experienced that there is a large difference between the combination of weights that are appropriate for designing local $\mathscr{H}_\infty$ controllers and the weights necessary for appropriate simulation results in the LPV framework. For the weights for the LPV control, it was necessary to exaggerate the weights to get the desired performance from a simulation point of view. This indicates that the assumption of arbitrarily fast parameter variations is conservative and it is therefore suggested to do similar investigations for rate-bounded parameter variations. The design algorithm in this case is in theory very similar, but the numerics are expected to be more difficult to handle, because conditioning of the design variables can vary more over the operating trajectory.

As a concluding remark it should be noted that model uncertainty is not handled directly in the design formulation, but the performance channels considering tower and drive train oscillations can be considered as a detuning of the tracking controller at the two respective eigenfrequencies. Also the channels from disturbance (wind speed) to control signals can be considered similar to the control sensitivity usually used in robust controller techniques. Robustness towards parametric uncertainty can be covered fairly well by sampling the parameter space.

ACKNOWLEDGEMENTS

The authors would like to thank Professor C. Scherer from Delft University of Technology, The Netherlands, for his helpful discussions about the numerics related to controller construction for LPV controllers.

REFERENCES

1. Gardner P, Garrad A, Jamieson P, Snodin H, Nichols G, Tindal A. Wind energy—the facts—volume 1. *Technical Report*, Garrad Hassan for European Wind Energy Association, 2002.
2. Hand MM, Balas MJ. Systematic controller design methodology for variable-speed wind turbines. *Technical Report*, NREL, 2002.
3. Vihriälä H, Ridanpää P, Perälä R, Söderlund L. Control of a variable speed wind turbine with feedforward of aerodynamic torque. *European Wind Energy Conference*, Nice, France, 1999; 881–884.
4. Connor B, Leithead WE, Grimble MJ. LQG control of a constant speed horizontal axis wind turbine. *Conference on Control Applications*, Glasgow, Scotland, 1994; 251–252. DOI: 10.1109/CCA.1994.381190.
5. Munteanu I, Cutululis NA, Bratcu AI, Ceanga E. Optimization of variable speed wind power systems based on a LQG approach. *Control Engineering Practice* 2004; **13**(7):903–912. DOI: 10.1016/j.conengprac.2004.10.013.
6. Rocha R, Filho LSM, Bortolus MV. Optimal multivariable control for wind energy conversion system—a comparison between $\mathscr{H}_2$ and $\mathscr{H}_\infty$ controllers. *Conference on Decision and Control*, Seville, Spain, 2005; 7906–7911.
7. Cutululis NA, Ceanga E, Hansen AD, Sørensen P. Robust multi-model control of an autonomous wind power system. *Wind Energy* 2006; **9**:399–419. DOI: 10.1002/we.194.
8. Jelavić M, Perić N, Petrović I, Car S, Maderčić M. Design of a wind turbine pitch controller for loads and fatigue reduction. *European Wind Energy Conference*, Milan, Italy, 2007.
9. Kraan I, Bongers PMM. Control of a wind turbine using several linear robust controllers. *Conference on Decision and Control*, San Antonio, TX, U.S.A., 1993; 1928–1929. DOI: 10.1109/CDC.1993.325530.
10. Leith DJ, Leithead WE. Application of nonlinear control to a HAWT. *Conference on Control Applications*, Glasgow, Scotland, 1994; 245–250. DOI: 10.1109/CCA.1994.381191.

11. Leith DJ, Leithead WE. Appropriate realization of gain-scheduled controllers with application to wind turbine regulation. *International Journal of Control* 1996; **65**(2):223–248. DOI: 10.1080/00207179608921695.
12. van Engelen TG, van der Hooft EL, Schaak P. Development of wind turbine control algorithms for industrial use. *European Wind Energy Conference*, Madrid, Spain, 2003.
13. Lescher F, Camblong H, Curea O, Briand R. LPV control of wind turbines for fatigue loads reduction using intelligent micro sensors. *American Control Conference*, New York City, NY, U.S.A., 2007; 6061–6066.
14. Lescher F, Zhao JY, Borne P. Robust gain scheduling controller for pitch regulated variable speed wind turbine. *Studies in Informatics and Control* 2005; **14**(4):299–315.
15. Mantz RJ, Bianchi FD, Christiansen CF. Gain scheduling control of variable-speed wind energy conversion systems using quasi-LPV models. *Control Engineering Practice* 2005; **13**:247–255. DOI: 10.1016/j.conengprac.2004.03.006.
16. Balas GJ. Linear, parameter-varying control and its applications to a turbofan engine. *International Journal of Robust and Nonlinear Control* 2002; **12**:763–796. DOI: 10.1002/rnc.704.
17. Burton T, Sharpe D, Jenkins N, Bossanyi EA. *Wind Energy Handbook*. Wiley: New York, 2001. DOI: 10.1002/0470846062.
18. Østeraard KZ, Brath P, Stoustrup J. Estimation of effective wind speed. *Journal of Physics*: *Conference Series* 2007; **75**. Available at: http://www.iop.org/EJ/toc/1742-6596/75/1.
19. Howze JW, Bhattacharyya SP. Robust tracking, error feedback, and two-degree-of-freedom controllers. *Transactions on Automatic Control* 1997; **42**(7):980–983.
20. Shamma JS, Athans M. Analysis of gain scheduled control for nonlinear plants. *Transactions on Automatic Control* 1990; **35**(8):898–907. DOI: 10.1109/9.58498.
21. Becker G, Packard A. Robust performance of linear parametrically varying systems using parametrically-dependent linear feedback. *Systems and Control Letters* 1994; **23**:205–215. DOI: 10.1016/0167-6911(94)90006-X.
22. Gahinet P, Apkarian P. A linear matrix inequality approach to $\mathscr{H}_\infty$ control. *International Journal of Robust and Nonlinear Control* 1994; **4**:421–448. DOI: 10.1002/rnc.4590040403.
23. Østergaard KZ. Robust, gain-scheduled control of wind turbines. *Ph.D. Thesis*, Aalborg University, 2008.
24. Helmersson A. IQC synthesis based on inertia constraints. *IFAC World Congress*, Beijing, China, 1999.
25. Scherer CW. *Recent Advantages on LMI Methods in Control*. Chapter: Robust mixed control and LPV control with full block scalings. SIAM: Philadelphia, PA, 2000.
26. Apkarian P, Gahinet P, Becker G. Self-scheduled $\mathscr{H}_\infty$ control of linear parameter-varying systems—a design example. *Automatica* 1995; **31**(9):1251–1261. DOI: 10.1016/0005-1098(95)00038-X.
27. Scherer CW. LPV control and full block multipliers. *Automatica* 2001; **37**:361–375.
28. Iwasaki T, Shibata G. LPV system analysis via quadratic separator for uncertain implicit systems. *Transactions on Automatic Control* 2001; **46**(8):1195–1208. DOI: 10.1109/9.940924.
29. Wu F, Yang XH, Packard A, Becker G. Induced $\mathscr{L}_2$-norm control for LPV system with bounded parameter variation rates. *American Control Conference*, Seattle, Washington, U.S.A., 1995; 2379–2383.
30. Gahinet P. Explicit controller formulas for LMI-based $\mathscr{H}_\infty$ synthesis. *Automatica* 1996; **32**(7):1007–1014. DOI: 10.1016/0005-1098(96)00033-7.
31. Trangbæk K. Linear parameter varying control of induction motors. *Ph.D. Thesis*, Aalborg University, 2001.
32. IEC. *IEC 61400-1*. International Standard, 2005.
33. Hammerum K. A fatigue approach to wind turbine control. *Master's Thesis*, Technical University of Denmark, 2006.